

COMPUTATIONALLY EFFICIENT MODELS OF URBAN AND NATURAL TERRAIN BY NON-ITERATIVE DOMAIN DECOMPOSITION FOR L_1 SMOOTHING SPLINES

Yu-Min Lin, Wei Zhang and Shu-Cherng Fang
Industrial Engineering and Operations Research
North Carolina State University
Raleigh, NC 27695

Yong Wang
SAS Institute Inc.
Cary, NC 27513

John E. Lavery*
Mathematics Division
Army Research Office, Army Research Laboratory
Research Triangle Park, NC 27709

ABSTRACT

In this paper, we propose and validate a computationally efficient *non-iterative* domain decomposition procedure for calculating bivariate cubic L_1 smoothing splines. This domain decomposition procedure involves calculating local L_1 smoothing splines individually on overlapping “extended subdomains” that cover the global domain and then creating the global L_1 smoothing spline by patching together the local L_1 smoothing splines. Using this procedure, we calculate the global L_1 smoothing splines of one urban terrain data set (Baltimore) and one natural terrain data set (Killeen, Texas). The local L_1 smoothing splines generally match well at subdomain boundaries but do not always do so. The current hypothesis is that the cases in which the local L_1 smoothing splines do not match well at the boundaries of the subdomains are due to limitations in the compressed primal-dual algorithm that is used to calculate the local L_1 smoothing splines. The non-iterative nature of this new domain decomposition procedure is in strong contrast to and is a large improvement over the iterative nature of all previously known domain decomposition procedures. With sequential and especially with parallel computation, the non-iterative L_1 smoothing spline domain decomposition procedure will be a large factor in reducing computing time so that complex terrain models can be calculated and manipulated in real time.

1. INTRODUCTION

Over the past five years, a number of publications have provided evidence that L_1 smoothing splines and related L_1 interpolating splines preserve the shape of urban and natural terrain well, better than any other type of spline (polynomial, rational, exponential or trigonometric). Cubic L_1 smoothing and interpolating

splines have been used to represent natural and urban terrain, geophysical features and financial processes (Champion and Lavery, 2002; Gilsinn and Lavery, 2002; Lavery, 2001, 2004; Lavery and Gilsinn, 2000, 2001; Wang et al., 2006) and can be used to represent other types of irregular data/functions such as geographical information, biological objects, mechanical objects, images, economic processes and social processes. L_1 interpolating splines have dominated the previous research on L_1 splines. However, L_1 interpolating splines have no compression capability. In contrast, L_1 smoothing splines do provide compression, at the expense of some loss of information, of course. Previously, L_1 smoothing splines have been calculated globally (Champion and Lavery, 2002; Gilsinn and Lavery, 2002). In this present paper, we investigate a new, non-iterative domain decomposition procedure for calculating L_1 smoothing splines and present computational results for urban and natural terrain. A related non-iterative domain decomposition procedure for L_1 interpolating splines is currently under development by the authors of this present paper.

2. COMPUTATIONAL MODEL

Bivariate cubic L_1 smoothing splines, proposed by Gilsinn and Lavery (2002), are defined by minimizing the functional

$$\alpha \sum_{m=1}^M \hat{w}_m |z(\hat{x}_m, \hat{y}_m) - \hat{z}_m| + (1 - \alpha) \iint_D \left[\left| \frac{\partial^2 z}{\partial x^2} \right| + 2 \left| \frac{\partial^2 z}{\partial x \partial y} \right| + \left| \frac{\partial^2 z}{\partial y^2} \right| \right] dx dy \quad (1)$$

Report Documentation Page

Form Approved
OMB No. 0704-0188

Public reporting burden for the collection of information is estimated to average 1 hour per response, including the time for reviewing instructions, searching existing data sources, gathering and maintaining the data needed, and completing and reviewing the collection of information. Send comments regarding this burden estimate or any other aspect of this collection of information, including suggestions for reducing this burden, to Washington Headquarters Services, Directorate for Information Operations and Reports, 1215 Jefferson Davis Highway, Suite 1204, Arlington VA 22202-4302. Respondents should be aware that notwithstanding any other provision of law, no person shall be subject to a penalty for failing to comply with a collection of information if it does not display a currently valid OMB control number.

| | | | | | |
|---|------------------------------------|-------------------------------------|----------------------------|--|---------------------------------|
| 1. REPORT DATE 01 NOV 2006 | | 2. REPORT TYPE N/A | | 3. DATES COVERED - | |
| 4. TITLE AND SUBTITLE Computationally Efficient Models Of Urban And Natural Terrain By Non-Iterative Domain Decomposition For L1 Smoothing Splines | | | | 5a. CONTRACT NUMBER | |
| | | | | 5b. GRANT NUMBER | |
| | | | | 5c. PROGRAM ELEMENT NUMBER | |
| 6. AUTHOR(S) | | | | 5d. PROJECT NUMBER | |
| | | | | 5e. TASK NUMBER | |
| | | | | 5f. WORK UNIT NUMBER | |
| 7. PERFORMING ORGANIZATION NAME(S) AND ADDRESS(ES) Industrial Engineering and Operations Research North Carolina State University Raleigh, NC 27695 | | | | 8. PERFORMING ORGANIZATION REPORT NUMBER | |
| 9. SPONSORING/MONITORING AGENCY NAME(S) AND ADDRESS(ES) | | | | 10. SPONSOR/MONITOR'S ACRONYM(S) | |
| | | | | 11. SPONSOR/MONITOR'S REPORT NUMBER(S) | |
| 12. DISTRIBUTION/AVAILABILITY STATEMENT Approved for public release, distribution unlimited | | | | | |
| 13. SUPPLEMENTARY NOTES See also ADM002075., The original document contains color images. | | | | | |
| 14. ABSTRACT | | | | | |
| 15. SUBJECT TERMS | | | | | |
| 16. SECURITY CLASSIFICATION OF: | | | 17. LIMITATION OF ABSTRACT | 18. NUMBER OF PAGES | 19a. NAME OF RESPONSIBLE PERSON |
| a. REPORT unclassified | b. ABSTRACT unclassified | c. THIS PAGE unclassified | | | |

Here, D is a 2D “global domain” over which a piecewise cubic L_1 smoothing spline $z(x, y)$ is to be calculated. The data to be approximated are \hat{z}_m given at locations (\hat{x}_m, \hat{y}_m) , $m = 1, 2, \dots, M$ with weights \hat{w}_m . The quantity α is a balance parameter that determines the trade-off between fitting the data, represented by the sum, and ensuring that the smoothing spline does not have extraneous oscillation, represented by the integral.

The cubic L_1 smoothing splines that we use in this paper are created on regularly spaced rectangular grids with nodes (x_i, y_j) , $i = 0, 1, \dots, I, j = 0, 1, \dots, J$, on the domain $D = (x_0, x_I) \times (y_0, y_J)$ and are based on Sibson elements (Han and Schumaker, 1997; Lavery, 2001). These smoothing splines are characterized by their elevation $z(x_i, y_j)$ and derivatives $\partial z(x_i, y_j)/\partial x$ and $\partial z(x_i, y_j)/\partial y$ at the nodes (x_i, y_j) . The elevations and derivatives are determined by minimizing functional (1). To carry out this minimization, we discretize functional (1) in the following manner. Divide each cell $(x_i, x_{i+1}) \times (y_j, y_{j+1})$ of D into K^2 equal subrectangles, $K \geq 2$. The integral over the cell is approximated by $1/2K(K-1)$ times the sum of the $2K(K-1)$ values of the integrand at the midpoints of the sides of the subrectangles that are in the interior of the rectangle. Minimization of the discretized version of (1) is a linear program that we solve using a compressed primal-dual algorithm (Wang et al., 2006). For the computational results in this present paper, we added a matrix re-ordering procedure to the compressed primal-dual algorithm to reduce the bandwidth of the reweighted least squares matrices that occur in this algorithm and thereby increase the size of the domains that the algorithm can handle.

Let L be a divisor of I and J . Divide the global domain D into equal subdomains of $L \times L$ cells. Except at the boundary of the global domain, extend each subdomain of $L \times L$ cells by E cells in all directions (top, bottom, right and left). This yields “extended subdomains” of $(L+2E) \times (L+2E)$ cells (linear dimension $L+E$ cells when a subdomain borders on the boundary of the global domain). The domain decomposition procedure consists of three steps, namely, 1) calculating the L_1 smoothing spline individually on each of the extended subdomains, 2) restricting the spline on each extended subdomain to the basic subdomain of $L \times L$ cells inside that extended subdomain and 3) creating the L_1 smoothing spline on the global domain D by patching together the L_1 smoothing splines on the $L \times L$ -cell subdomains. In contrast to all previous domain decomposition procedures, this procedure is *non-iterative*, that is, it does not require that information be transferred between subdomains and that Step 1 be repeated. Previous domain decomposition procedures cannot be

non-iterative because the minimization principles were such that a change in the data at any point in the global domain affects the smoothing spline everywhere in the global domain. In contrast, a change in the data at a given point affects the L_1 smoothing spline only in a limited region around that point. Thus, L_1 smoothing splines can be calculated by a non-iterative domain decomposition procedure as long as L and E are sufficiently large. Determining appropriate L and E is a critical issue in implementing an L_1 smoothing spline domain decomposition procedure. We consider this issue in the next section.

We will present computational results for three artificial data sets and two real-terrain data sets. The three artificial data sets all consist of 641×641 points on an equally spaced rectangular grid. The first artificial data set has data with height 0 to the left of a north-south line through the center of the xy grid of this data set and height 1 on and to the right of this line. The second artificial data set has data with height 0 to the left of a northeast-southwest diagonal line through the center of the xy grid of this data set and height 1 on and to the right of this line. The third artificial data set has data with height 0 and 1 alternatively for every 10 rows of the xy grid. The first real-terrain data set is an urban terrain data set consisting of 1000×1000 points of 1m-spacing data for Baltimore, MD provided by the Joint Precision Strike Demonstration Project Office (JPSD PO) Rapid Terrain Visualization (RTV) ACTD. The second real-terrain data set is a natural-terrain data set consisting of 1201×1201 points of DTED1 (100m spacing) data for Killeen, Texas provided by the National Geospatial-Intelligence Agency. The urban-terrain and natural-terrain data sets were previously used in (Champion and Lavery, 2002; Lavery, 2001, 2004; Lavery and Gilsinn, 2000, 2001; Wang et al., 2006).

In all of the computational experiments in this paper, there are $9 \times 9 = 81$ points in each closed cell $[x_i, x_{i+1}] \times [y_j, y_{j+1}]$. For very large domains, the “raw compression ratio”, that is the number of degrees of freedom in the data divided by the number of degrees of freedom in the L_1 smoothing spline is therefore $8^2/3 = 21.33$. For all the computation results in this paper, $K = 3$ and $\hat{w}_m = 1$ for $m = 1, 2, \dots, M$.

3. DETERMINING SIZES OF SUBDOMAINS AND EXTENDED SUBDOMAINS

3.1 Relation between E and L

To establish a relation between E and L , we will calculate the E that minimizes the computational cost of the domain decomposition procedure on a sequential computer. In the compressed primal-dual algorithm that we use to calculate L_1 splines, the computational cost is

dominated by the cost of the factorization of the symmetric reweighted least-squares matrix on each iteration of this algorithm. (The number of iterations of the compressed primal-dual algorithm for L_1 smoothing splines is roughly independent of the size of the domain/subdomain and is not a factor here.) Without loss of generality, assume that $J \leq I$. For a global domain of $I \times J$ cells, there are $3(I+1) \times (J+1)$ unknowns ($z(x_i, y_j)$, $\partial z(x_i, y_j)/\partial x$ and $\partial z(x_i, y_j)/\partial y$ at each node (x_i, y_j)), the number of superdiagonals (and subdiagonals) in the least-squares matrix is $3J + 9$ and the factorization of this reweighted, least-squares matrix therefore costs, to highest order, $243IJ^3$ flops. For each extended subdomain of $(L+2E) \times (L+2E)$ cells, there are $3(L+2E+1)^2$ unknowns, the number of superdiagonals in the least-squares matrix of the compressed primal-dual algorithm is $3L+6E+9$ and the factorization of this matrix costs, to highest order, $243(L+2E)^4$ flops. The total operation count on a sequential computer for the $(I/L) \times (J/L)$ subdomains is therefore $243(L+2E)^4(I/L)(J/L)$. With I , J and L fixed, the minimum of this expression occurs when $E=L/2$. We will use this relation as a basis for the computational experiments reported in Subsec. 3.2 below.

3.2 Determining E from Computational Experiments

For the domain decomposition procedure outlined in Sec. 2 to perform non-iteratively as claimed, the “width” E of the ring around each subdomain needs to be large enough that the L_1 smoothing spline on the basic subdomain of $L \times L$ cells inside the extended subdomain is independent of the data outside of the extended subdomain. To determine how large E needs to be, we conduct a series of computational experiments to determine how far a perturbation in the data propagates in the L_1 smoothing spline.

In all of the computational experiments in this subsection, the total number of data points is 641^2 , the size of the domain D is 80×80 cells (which corresponds to $L = 40$, $E = L/2 = 20$) and there are (as previously stated) $9 \times 9 = 81$ points in each closed cell. For one set of computational experiments, we created a perturbation by adding a constant p to the heights at the 9×9 points at the center of the data set. In another set of computational experiments, we added a constant p to the heights at a set of 9×9 points at a corner. To determine the distance that a perturbation in the data propagates in an L_1 smoothing spline, we compare the L_1 smoothing spline of the perturbed data with the L_1 smoothing spline of the original data. Differences in heights at the nodes are considered significant (“nonzero”) if they are, in absolute value, $\geq 10^{-3}p$. (The level $10^{-3}p$ is consistent with the

numerical accuracy of the compressed primal-dual algorithm used to calculate L_1 smoothing splines.)

We carried out 3 sets of computational experiments with, respectively, the first, second and third artificial data sets, each with balance parameter $\alpha = 0.05, 0.1$ and 0.2 . We also carried out 2 sets of computational experiments with a 641×641 portion of the urban terrain data set and 2 sets of computational experiments with a 641×641 portion of the natural terrain data set, each with $\alpha = 0.05, 0.1$ and 0.2 . In these computational experiments, the minimum, median, average and maximum distances propagated by the perturbation in the L_1 smoothing splines were 0, 4, 12.19 and 40 cells, respectively. When the optimal α was chosen, the minimum, median, average and maximum distances propagated by the perturbation in the L_1 smoothing splines were 0, 2, 5.07 and 11, respectively. (The optimal α value can be different for different data sets.) In the following, we present results of computational experiments for the Baltimore data set with $p = 100$ and $\alpha = 0.2$ and for the Killeen data set with $p = 200$ and $\alpha = 0.2$.

Figures 1a and 1b are the original surface and the L_1 smoothing spline, respectively, for the Baltimore data.

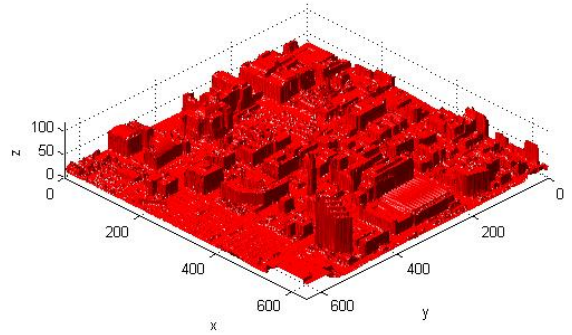


Fig. 1a. 641×641 portion of Baltimore data set

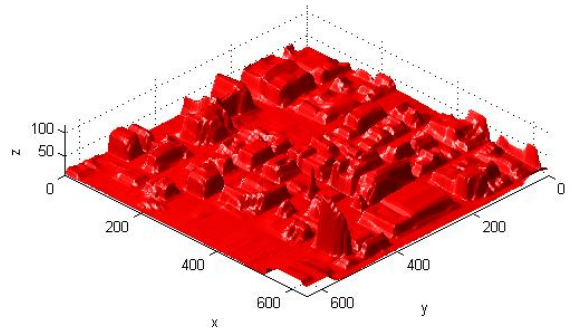


Fig. 1b. L_1 smoothing spline for 641×641 portion of Baltimore data set

Figures 2a and 2b are the original surface and the L_1 smoothing spline, respectively, for the Baltimore data with the perturbation at the center of the data. Fig. 3 is the difference between the L_1 smoothing spline with the perturbation, shown in Fig. 2b, and the L_1 smoothing spline without the perturbation, shown in Fig. 1b.

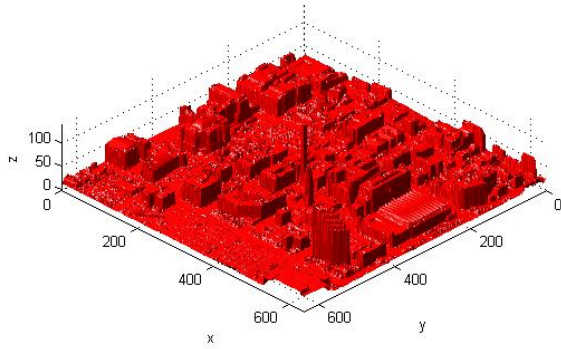


Fig. 2a. 641×641 portion of Baltimore data set with perturbation at center

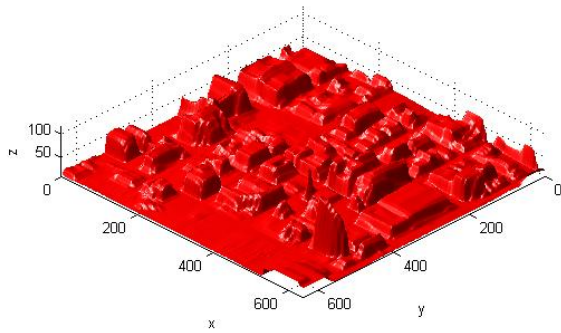


Fig. 2b. L_1 smoothing spline for 641×641 portion of Baltimore data set with perturbation at center

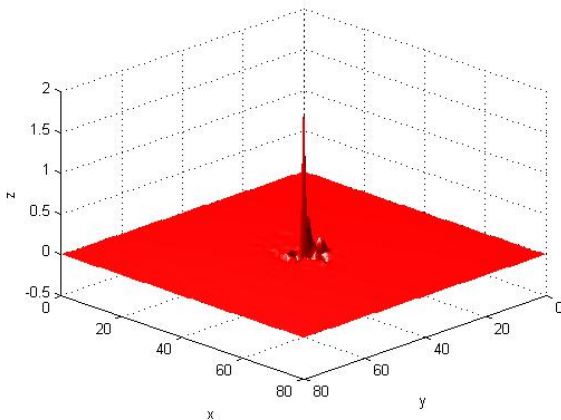


Fig. 3. Difference between the L_1 smoothing splines of Figs 2b and 1b

Figures 4a and 4b are the original surface and the L_1 smoothing spline, respectively, for the Baltimore data with the perturbation at a corner of the data. Fig. 5 is the difference between the L_1 smoothing spline with the perturbation, shown in Fig. 4b, and the L_1 smoothing spline without the perturbation, shown in Fig. 1b.

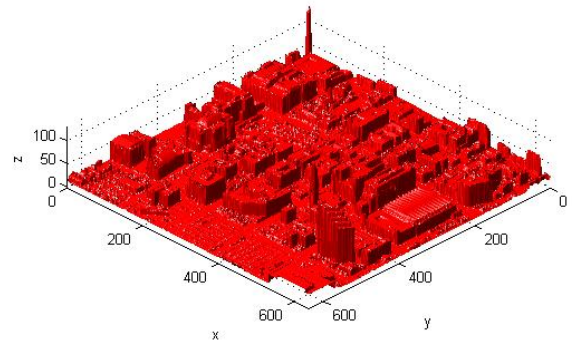


Fig. 4a. 641×641 portion of Baltimore data set with perturbation at corner

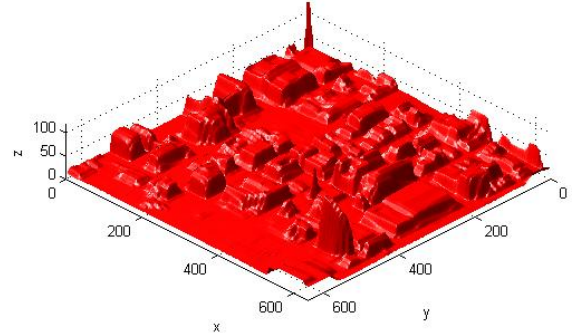


Fig. 4b. L_1 smoothing spline for 641×641 portion of Baltimore data set with perturbation at corner

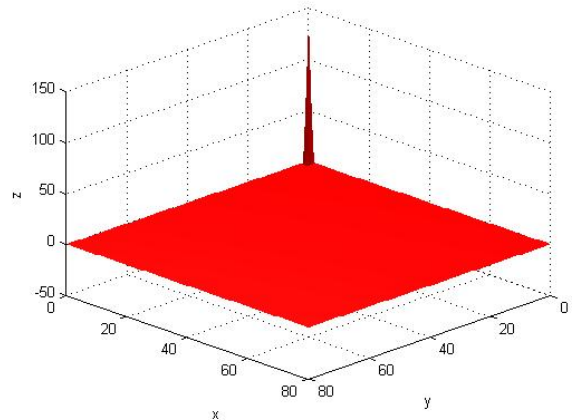


Fig. 5. Difference between the L_1 smoothing splines of Figs 4b and 1b

Figures 6a and 6b are the original surface and the L_1 smoothing spline, respectively, for the Killeen data.

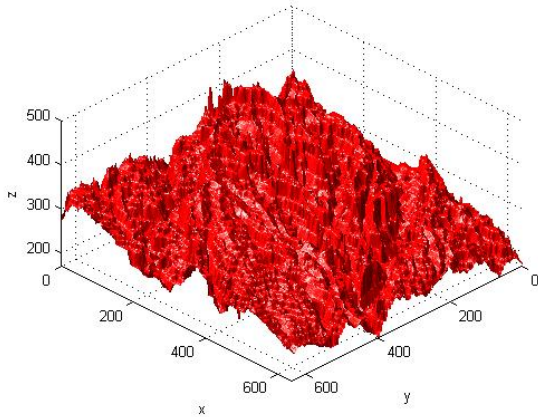


Fig. 6a. 641×641 portion of Killeen data set

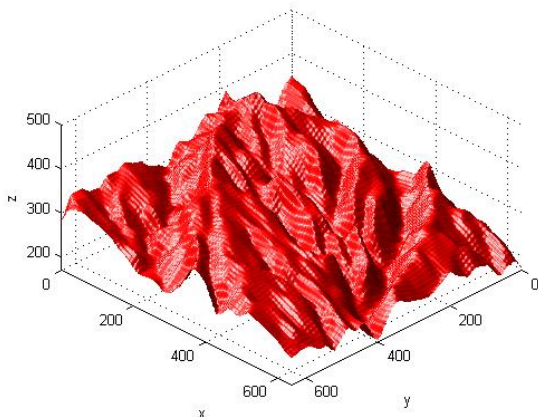


Fig. 6b. L_1 smoothing spline for 641×641 portion of Killeen data set

Figures 7a and 7b are the original surface and the L_1 smoothing spline, respectively, for the Killeen data with the perturbation at the center of the data. Fig. 8 is the difference between the L_1 smoothing spline with the perturbation, shown in Fig. 7b and the L_1 smoothing spline without the perturbation, shown in Fig. 6b. Figures 9a and 9b are the original surface and the L_1 smoothing spline, respectively, for the Killeen data with the perturbation at a corner of the data. Fig. 10 is the difference between the L_1 smoothing spline with the perturbation, shown in Fig. 9b and the L_1 smoothing spline without the perturbation, shown in Fig. 6b.

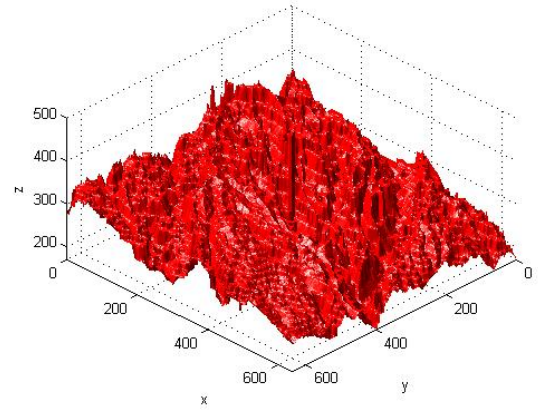


Fig. 7a. 641×641 portion of Killeen data set with perturbation at center

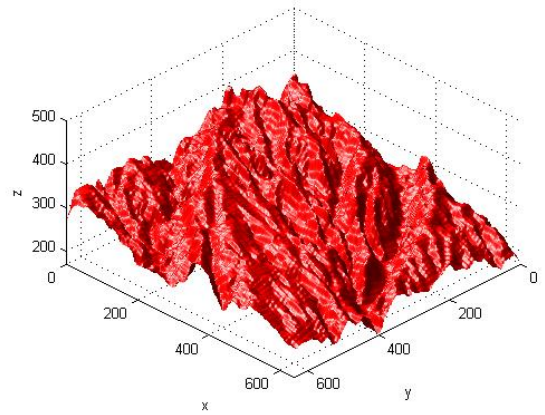


Fig. 7b. L_1 smoothing spline for 641×641 portion of Killeen data set with perturbation at center

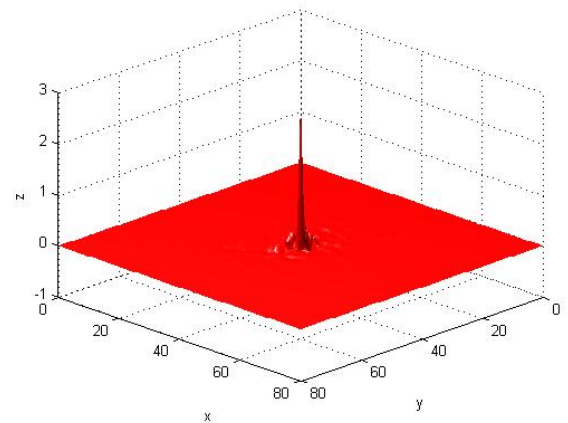


Fig. 8. Difference between the L_1 smoothing splines of Figs 7b and 6b

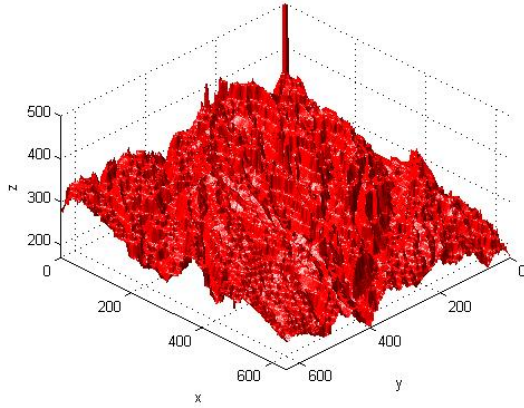


Fig. 9a. 641×641 portion of Killeen data set with perturbation at corner

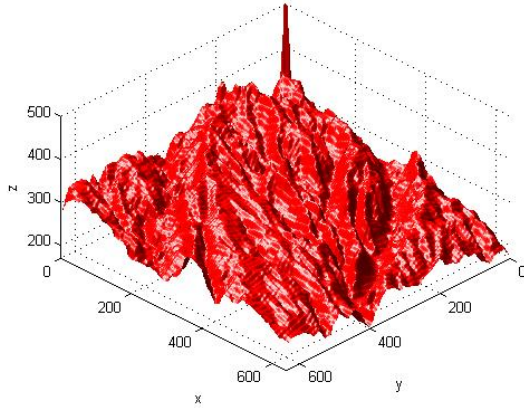


Fig. 9b. L_1 smoothing spline for 641×641 portion of Killeen data set with perturbation at corner

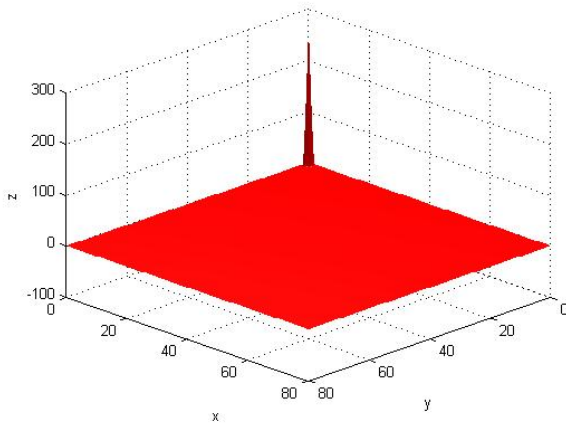


Fig. 10. Difference between the L_1 smoothing splines of Figs 9b and 6b

In Figs., 3, 5, 8 and 10, the significant differences, that is, those $\geq 10^{-3} p$ in absolute value, occur at most 6

cells distant from the locations of the perturbations in Figs. 2a, 4a, 7a and 9a.

4. COMPUTATIONAL RESULTS FOR URBAN AND NATURAL TERRAIN

So that the ring by which each subdomain is extended is large enough to assure that the L_1 smoothing spline in that subdomain is not affected by the data outside the extended subdomain, we need to choose E to be greater than the maximum of 6 cells that the perturbation propagates in Figs. 3, 5, 8 and 10 and greater than the maximum of 15 cells that the perturbation propagates in the other computational experiments reported at the beginning of Subsec. 3.2. We choose $E = 20$. We use the optimal $\alpha = 0.2$.

We first calculate the global L_1 smoothing spline for a 993×993 portion of the Baltimore data set, depicted in Fig. 11a, by domain decomposition. We set up a smoothing spline grid of 124×124 equal cells that precisely covers the 993×993 data grid. We divide the smoothing spline grid into four subdomains, each of 62×62 cells ($L = 62$), that overlap only at their boundaries. We calculate the local L_1 smoothing splines on each of the four extended subdomains of size 82×82 and then create the global L_1 smoothing spline by patching together the four local L_1 smoothing splines. Numerical errors in the compressed primal-dual algorithm result in the four local L_1 smoothing splines not matching exactly on overlapping boundaries. The minimum, median, average and maximum of the absolute values of the differences of the z , $\partial z/\partial x$ and $\partial z/\partial y$ at the smoothing spline nodes on overlapping subdomain boundaries are given in Table 1.

Table 1. Minimum, median, average and maximum of the absolute values of the differences of quantities on overlapping subdomain boundaries for Baltimore data.

| | Min | Median | Average | Max |
|-----------------------------------|-----|--------|---------|--------|
| $z(x_i, y_j)$ | 0 | 0.0071 | 0.1575 | 2.6137 |
| $\partial z(x_i, y_j)/\partial x$ | 0 | 0.0027 | 0.0602 | 1.3892 |
| $\partial z(x_i, y_j)/\partial y$ | 0 | 0.0008 | 0.0250 | 1.5404 |

As the data in Table 1 indicates, the differences in z , $\partial z/\partial x$ and $\partial z/\partial y$ at the smoothing spline nodes on overlapping subdomain boundaries are generally small compared to the total difference in elevation of 100 in the Baltimore data set. The maximum absolute differences of 2.6137, 1.3892 and 1.5404 in z and its derivatives need to be investigated further to determine whether they are due to numerical limitations of the compressed primal-dual algorithm or to some other cause. When patching the local L_1 smoothing splines together to create the global L_1

smoothing splines, we resolve the (generally only slight) differences in z , $\partial z/\partial x$, and $\partial z/\partial y$ at the nodes on overlapping subdomain boundaries by averaging the two or more values of each quantity at each node. In Fig. 11b, we present the global L_1 smoothing spline calculated by domain decomposition for the 993×993 portion of the Baltimore data set.

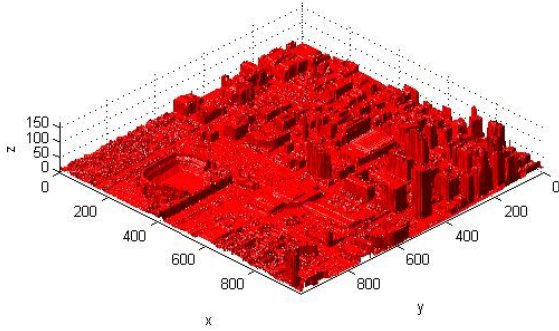


Fig. 11a. 993×993 portion of Baltimore data set

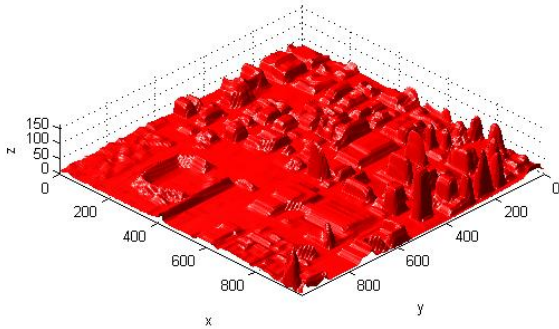


Fig. 11b. L_1 smoothing spline calculated by domain decomposition for 993×993 portion of Baltimore data set

We also calculate the global L_1 smoothing spline for the Killeen data set, depicted in Fig. 12a, by domain decomposition. We set up a smoothing spline grid of 150×150 equal cells that precisely covers the 1201×1201 data grid. We divide the smoothing spline grid into nine subdomains, each of 50×50 cells ($L = 50$), that overlap only at their boundaries. We calculate the local L_1 smoothing splines on each of the four extended subdomains of size 70×70 cells (at corners), the four extended subdomains of size 70×90 cells (on boundaries of the global domain but not at a corner) and the one extended subdomain of size 90×90 cells (in the interior) and then create the global L_1 smoothing spline by patching together the nine local L_1 smoothing splines on the basic subdomains inside these extended subdomains. The minimum, median, average and maximum of the absolute values of the differences of the z , $\partial z/\partial x$ and $\partial z/\partial y$

at the smoothing spline nodes on overlapping subdomain boundaries are given in Table 2.

Table 2. Minimum, median, average and maximum of the absolute values of the differences of quantities on overlapping subdomain boundaries for Killeen data.

| | Min | Median | Mean | Max |
|-----------------------------------|-----|--------|--------|--------|
| $z(x_i, y_j)$ | 0 | 0.1600 | 0.3556 | 4.2500 |
| $\partial z(x_i, y_j)/\partial x$ | 0 | 0.0320 | 0.0899 | 1.1394 |
| $\partial z(x_i, y_j)/\partial y$ | 0 | 0.0280 | 0.0703 | 1.4139 |

As was the case for the data in Table 1, the data in Table 1 indicates that the differences in z , $\partial z/\partial x$ and $\partial z/\partial y$ at the smoothing spline nodes on overlapping subdomain boundaries are generally small compared to the total difference in elevation of 230 in the Killeen data set but the maximum absolute differences of 4.2500, 1.1394 and 1.4139 need to be investigated further. Averaging the (generally only slightly) different values of z , $\partial z/\partial x$, and $\partial z/\partial y$ at the nodes on overlapping subdomain boundaries, we produce the global L_1 smoothing spline calculated by domain decomposition for the Killeen data set presented in Fig. 12b.

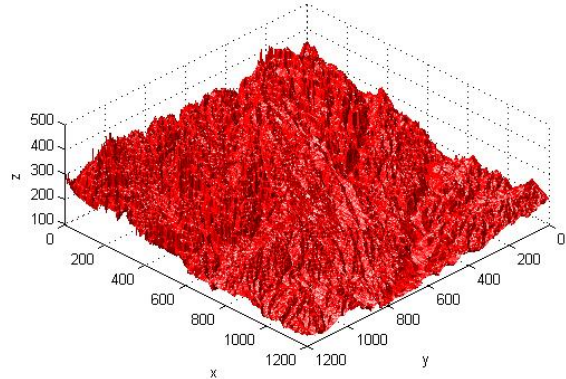


Fig. 12a. 1201×1201 Killeen data set

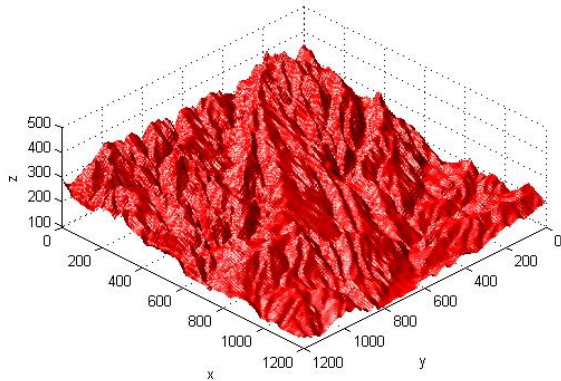


Fig. 12b. L_1 smoothing spline calculated by domain decomposition for Baltimore data set

5. CONCLUSION

The computational results presented in this paper indicate considerable success in designing a new non-iterative domain decomposition procedure and also indicate an open question. The local L_1 smoothing splines generally match well at subdomain boundaries but do not always do so. The current hypothesis is that the cases in which the L_1 smoothing splines do not match well at the boundaries of the subdomains are due to limitations in the compressed primal-dual algorithm. Whether this hypothesis is correct or not will be a topic of future research.

The non-iterative domain decomposition procedure for L_1 smoothing splines introduced in this paper reduces a minimization problem on the global domain to a set of disjoint minimization problems on overlapping “extended subdomains” and thereby reduces the computational load—by orders of magnitude if the global domain is large and there are a large number of small extended subdomains. The non-iterative nature of this domain decomposition procedure is in strong contrast to and is a large improvement over the iterative nature of all previously known domain decomposition procedures for splines and for elliptic partial differential equations. If successful, this domain decomposition procedure will allow L_1 smoothing splines to be used for compression in urban and natural terrain models. With sequential and especially with parallel computation, the non-iterative L_1 smoothing spline domain decomposition procedure will be a large factor in reducing computing time so that complex terrain models can be calculated and manipulated in real time.

REFERENCES

- Champion, D.C., and J.E. Lavery, 2002: Line of sight in natural terrain determined by L_1 -spline and conventional methods, in *Proc. 23rd Army Science Conf.*, Dept. Army, Washington, DC, OP-09.
- Gilsinn, D.E., and J.E. Lavery, 2002: Shape-preserving, Multiscale fitting of bivariate data by cubic L_1 smoothing splines, in Chiu, C.K., et al. (eds.), *Approximation Theory X: Wavelets, Splines, and Applications*, Vanderbilt University Press, Nashville, Tennessee, 283–293.
- Han, L., and L.L. Schumaker, 1997: Fitting monotone surfaces to scattered data using C^1 piecewise cubics, *SIAM J. Numer. Anal.* **34**, 569–585.
- Lavery, J.E., 2001: Shape-preserving, multiscale interpolation by bi- and multivariate cubic L_1 splines, *Comput. Aided Geom. Design* **18**, 321–343.
- Lavery, J.E., 2004: The state of the art in shape preserving, multiscale modeling by L_1 splines, in M.L. Lucian and M. Neamtu (Eds.), *Proc. SIAM Conf. Geom. Design Computing*, Nashboro Press, Brentwood, TN, pp. 365–376.
- Lavery, J.E., and D.E. Gilsinn, 2000: Multiresolution representation of urban terrain by L_1 splines, in *Proc. 22nd Army Sc. Conf.*, Dept. Army, Washington, DC (2000), 767–773.
- Lavery, J.E., and D.E. Gilsinn, 2001: Representation of natural terrain by cubic L_1 splines, in K. Kopotun et al. (eds.), *Trends in Approx. Th.*, Vanderbilt U. Press, Nashville, 235–242.
- Wang, Y., S.-C. Fang and J.E. Lavery, 2006: A compressed primal-dual method for bivariate cubic L_1 splines, *J. Comput. Appl. Math.*, to appear.